RSC Advances

REVIEW

View Article Online
View Journal | View Issue

Cite this: *RSC Adv.*, 2023, **13**, 13698

Selectivity of reaction pathways for green diesel production towards biojet fuel applications

Zeni Rahmawati,[a] Liangga Santoso,[a] Alan McCue,[b] Nor Laili Azua Jamari,[c] Sri Yayu Ninglasari,[d] Triyanda Gunawan[a] and Hamzah Fansuri[a]

Received 6th April 2023
Accepted 10th April 2023

DOI: 10.1039/d3ra02281a

rsc.li/rsc-advances

Green diesel is the second generation biofuel with the same structure as fossil fuels (alkanes), allowing this biofuel to provide excellent fuel properties over biodiesel such as higher energy content and lower hazardous gas emission. Generally, green diesel can be produced through the deoxygenation/hydrogenation of natural oil and/or its derivatives at 200–400 °C and 1–10 MPa over supported metal catalysts. This process comprises of three reaction pathways: hydrodeoxygenation, decarboxylation, and decarbonylation. The extent to which these three different pathways are involved is strongly influenced by the catalyst, pressure, and temperature. Subsequently, the determination of catalyst and reaction condition plays a significant role owing to the feasibility of the process and the economic point of view. This article emphasizes the reaction pathway of green diesel production as well as the parameters influencing the predominant reaction route.

1. Introduction

The consumption of fossil fuel has been increasing day by day, as shown by the use of 76 quadrillion British thermal units (Btu) of non-renewable fuel in 2021 and 33 quadrillion Btu per May 2022.[1] By 2050, the global use of fossil fuel is forecasted to reach 800 quadrillion Btu where industrial sector accounts for 50.9% followed by transportation with 27.9%. This elevating consumption of fossil fuel causes an adverse effect on the environment and the depletion of petroleum storage.[2]

As consequence, the high energy demand urges the development of renewable energy resource to address the issues related to fossil fuels. Many studies have been attempted to shift the non-renewable energy to the sustainable sources such as electrification, clean hydrogen and its derivatives, as well as renewable energy in the form of wind, solar, and biofuels. Among those alternatives, biofuel is projected as the most promising one for the reasons of feasible application and ability in particular areas such as aviation.[3–5]

Biofuel is classified into categories based upon the raw material: first, second, third, and fourth generation. The first generation is the conventional biofuel produced from food crops, including biodiesel through the esterification or transesterification of natural oil and animal fats. This generation also comprises bioethanol *via* fermentation process.[6] Second generation biofuel is synthesized from non-edible feedstock and organic waste. This second generation involves the production of biofuel with the same structure as fossil fuel such as green diesel.[7–11] The third generation biofuel refers to the biodiesel generated from microalgae.[12] Lastly, the fourth generation biofuel refers to the metabolism of genetically modified algae.[13]

In terms of productivity, fourth generation biofuel exhibited a promising superiority with 20–300 folds production above traditional biomass crops in a shorter harvesting cycle. It also performs high photosynthesis efficiency and requires lower bioproductive land as well as freshwater supplies. Despite those advantages, this type of biofuel shows several drawbacks associated with the high production cost, insufficient biomass production, human health and environmental risk.[14] The first and third generation biofuel provides several advantages in terms of the practicality of the process and the fuel properties. Transesterification reaction has very simple procedure under mild condition. Biodiesel is nontoxic, biodegradable, and having a high cetane number between 49–60.[15] The exhaust gas from biodiesel combustion contains no SO_x and relatively small amounts of CO.[16] Aside of those excellent properties, biodiesel exhibits several downsides compared to fossil fuel. High oxygen content of biodiesel causes an incomplete combustion, leading to an accumulation of carbon in the engine, filter and nozzles. Therefore, biodiesel is unable to be applied directly to the engine without mixing with fossil fuel. In addition, degradation of properties proceeds during the storage due to oxidation and

[a]*Department of Chemistry, Faculty of Science and Data Analytics, Institut Teknologi Sepuluh Nopember, Keputih, Sukolilo, Surabaya 60111, Indonesia. E-mail: zeni.rahmawati@its.ac.id*

[b]*Department of Chemistry, University of Aberdeen, Aberdeen AB24 3UE, UK*

[c]*Department of Chemistry & Biology, Centre of Defence Foundation Studies, National Defence University of Malaysia, Kem Sungai Besi, Kuala Lumpur 57000, Malaysia*

[d]*Department Business Management, Faculty of Creative Design and Digital Business, Institut Teknologi Sepuluh Nopember, Keputih, Sukolilo, Surabaya 60111, Indonesia*

polymerization.[17–19] These challenges can be addressed by green diesel or renewable hydrocarbon.

Green diesel is the second generation of biofuel having the same structure as fossil fuels (alkanes) and has the ability to reduce greenhouse gas emission.[20] Green diesel increases the Green House Gas (GHG) saving up to 60% higher compared to the Renewable Energy Use Directive (RED) reduction target. This value has not been achieved by the first generation of biofuel.[21]

Green diesel has been extensively studied and developed globally. Multinational company called Neste has become the main capitol of green diesel production in Europe, with production capacity of 3.37 billion litres per year.[5] USA produces about 960 million gallons of renewable diesel annually, which are used for Sustainable Aviation Fuel (SAF).[22] In Indonesia, the development of green diesel for biojet fuel has just started recently even though the initiative has emerged since 2013 through Indonesia Aviation Biofuels and Renewable Energy Task Force.[23] Biojet fuel performed a debut in Indonesia by the application of J.24 (Jet fuel containing 2.4% bioavtur from palm oil) to CN 235-22 plane that flew 10 000 feet above West Java in September 2021.[24] However, this development was behind the time according to some media and global organisation focused on renewable energy. This opinion was derived upon the fact that many kinds of biojet feedstock such as natural oils and biodiesel abundantly present in Indonesia.

Green diesel can be produced from vegetable oil through deoxygenation reaction. Mostly, the reaction is conducted at 200–400 °C and 1–10 MPa over supported metal catalysts.[25] Fatty acids and fatty acid methyl esters (FAME or biodiesel) are also employed as the feedstock noting that natural oil deoxygenation comprises of complicated steps. Fatty acid methyl ester is preferable since the transesterification of natural oil to produce FAME is more feasible than oil splitting to generate fatty acid. Furthermore, deoxygenation of biodiesel enables the oxygen removal leading to excellent fuel properties.[26]

Green diesel production involves several reactions including hydrodeoxygenation (HDO), decarboxylation (DCO_2) and decarbonylation (DCO). Hydrodeoxygenation removes oxygen *via* hydrogen insertion. This route produces water and hydrocarbons with the same carbon number as the feedstock.[27] In decarboxylation pathway, oxygen is released by discharging CO_2 resulting hydrocarbons with one less carbon atom. Meanwhile, decarbonylation eliminates oxygen from fatty acid through CO formation in the presence of hydrogen.[28] The extent to which these three different pathways involved is strongly influenced by the catalyst, pressure, and temperature.[29]

The selectivity of HDO and DCO/DCO_2 pathways is beneficial to observe since the route of desired hydrocarbon is associated to the reaction condition leading to the production cost and energy considerations.[30,31] For example, HDO requires more hydrogen while DCO/DCO_2 proceeds at higher temperature. Moreover, the products also meet the fuel properties: higher carbon in green diesel demonstrates higher cetane number and a lower ignition delay.

In this paper, the selectivity of HDO and DCO/DCO_2 routes in green diesel production will be discussed based upon the catalyst design and reaction conditions. This review also provides a profound outlook through a bibliometric study as well as the future challenges in this area, which still unavailable in other reviews as far.

2. Green diesel outlook: a bibliometric study

The bibliometric analysis provides green diesel outlook and its development through the years. The data was collected from Scopus database with the following sequence of query: TOPIC = Green diesel, LANGUAGE = English, timespan: 1972–2023, and keyword: 5 words. Without refining the data, 3150 sources were obtained from three categories: articles, reviews, and proceedings. The bibliometric analysis result was defined on the number of articles per year, sources, country, and citation network. The VOSviewer was selected to analyse this result.

The number of article related to green diesel per years was depicted in Fig. 1. The term green diesel was firstly considered through two articles published in 1972. Afterwards, this research area gained a very slight interest in a consistent number within 5 articles per year till 2000. Beyond this point, the number of published articles associated with green diesel continuously heightened up to 372 in 2022, affirming the enormous importance of green diesel as the promising renewable energy source.

The enormous interest on green diesel research was spread all over the world as depicted in Fig. 2. Among 3150 articles, the highest studies (544) were conducted in India, followed by the US with 431 articles. China was positioned at third highest contributor with 372 articles and Malaysia run afterward with 197 articles. Below that, various countries also generated articles with variety of article numbers.

In the span of 50 years, these 3150 articles related to green diesel have been published in various journals. In general, the authors opted to report green diesel studies in several journals related to the fuel, sustainable energy, green chemistry, environment, biomass and bioconversion. The articles akin to green

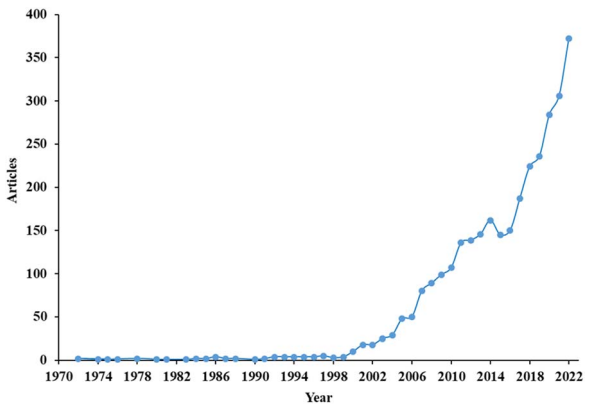

Fig. 1 The number of articles on green diesel studies published in the span on 1972–2022.

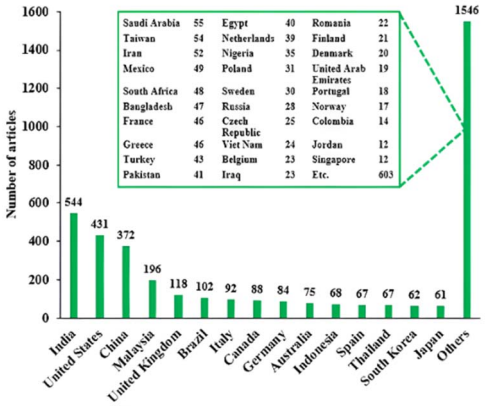

Fig. 2 The origin of green diesel studies published in various journals.

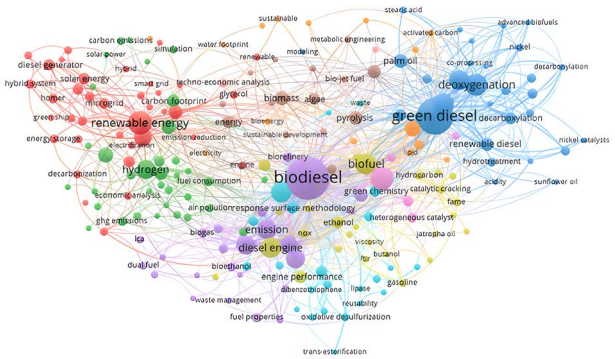

Fig. 3 Citation network on bibliometric result of green diesel studies.

diesel without noting the exact term was not included for the purpose of simplification.

A profound bibliographical study based upon the abstract key words was conducted as illustrated in Fig. 3. In terms of green diesel, the most mentioned keywords were related to the reaction pathways, feedstock, catalyst, and its function (blue line and dots). Deoxygenation was the highest mentioned keyword since it is the main reaction to produce green diesel with several reaction pathways such as decarboxylation and decarbonylation. Similar term such as co-processing and hydrotreatment were also used in several articles with palm oil as well as stearic acid were usually employed as the feedstock. The supported nickel was the most employed catalyst in green diesel production and activated carbon was the common support for the catalyst. Green diesel function as the renewable diesel was confirmed by the interrelated keywords of green diesel–biofuel–biodiesel (blue-yellow-purple lines and dots). Together with biodiesel, green diesel is very promising biofuel as renewable energy source, where green diesel enables the upgrade the biodiesel to the second generation biofuel apart from other feedstocks such as natural oil and its derivatives. The specific application of green diesel as biojet fuel was also highlighted since long chain alkanes was the predominates result. Subsequently, it is beneficial to investigate the route of

Table 1 Physico-chemical properties of biodiesel and green diesel[6]

Fuel properties	Unit	Biodiesel	Green diesel
Density	kg m^{-3}	880	790
Viscosity at 40 °C	mm^2 s^{-1}	2.9–11	2–4
Flash point	°C	100–180	59–138
Low heating value	MJ kg^{-1}	37.2–38	43.7–44.5
Cetane number		45–65	70–90
Oxygen	wt%	11.2	0

green diesel production and the parameter influencing the conversion as well as the alkane selectivity.

3. Green diesel

Green diesel, a second generation of biofuel with an alkane structure of fossil fuels, meets all the criteria for biofuel which is renewable, widely available, well distributed around the world, and has the potential to lower the greenhouse gaseous emissions.[26,32–35] The biofuel can be prepared from low quality feedstock with high fatty acid content that causes saponification reaction in biodiesel synthesis.

The most advantage of green diesel lays on the superior fuel properties over biodiesel. It fulfills the standard of ASTM D-975 regarding the density, viscosity, and cetane number.[31] Moreover, the study of emission and fuel consumption of green diesel and biodiesel tested by heavy duty diesel inferred that green diesel has better performance in the reduction of NO_x and lower fuel consumption.[6] Green diesel generated NO_x emission of 6.64 g kW^{-1} h^{-1}.[36] Table 1 shows the properties comparison between biodiesel and green diesel.

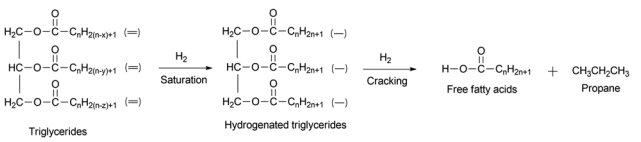

Fig. 4 Reaction pathway for free fatty acids production from triglycerides.

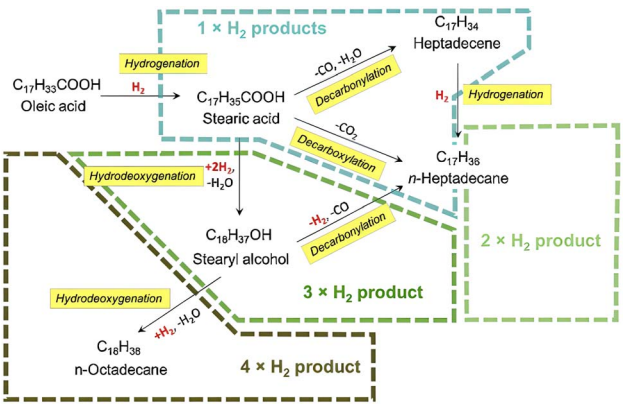

Fig. 5 Reaction pathway for green diesel production from fatty acid.

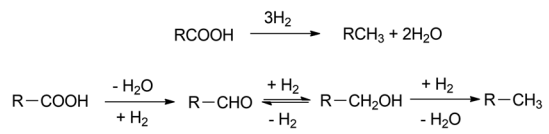

Fig. 6 Several steps of hydrodeoxygenation route.

Generally, green diesel can be produced from natural oil through deoxygenation reaction at 200–400 °C and 1–10 MPa over metal catalysts.[37–41] The initial step of deoxygenation is the hydrogenation of fatty ester or fatty acid containing double bonds, due to the reactivity of double bond being thermodynamically higher than the acid group.[42] This step is followed by the cracking of hydrogenated triglycerides to produce free fatty acids (Fig. 4).

Afterwards, free fatty acid is converted to alkanes through the hydrodeoxygenation, decarboxylation and decarbonylation pathways (Fig. 5).[43] The main reaction pathway is associated to the catalysts and reaction condition.

4. Hydrodeoxygenation

Hydrodeoxygenation (HDO) removes oxygen from fatty acids by insertion of hydrogen resulting hydrocarbons with the same carbon number as feedstock. This route is very efficient yet unpreferable sometimes, considering the requirement of high pressure of hydrogen.[44] In addition, this pathway consists of several intermediates such as aldehydes and fatty alcohols (Fig. 6). Subsequently, this route is also adopted to produce fatty alcohol by a manipulation on certain reaction conditions and catalyst. Nevertheless, HDO is mostly adopted in green diesel production at industrial scale such as Neste oil from the refinery in Porvoo, Finland.[45]

5. Decarboxylation/decarbonylation

Deoxygenation term will be frequently use in this section to indicate the process of oxygen removal which reflecting hydrodeoxygenation, decarboxylation and decarbonylation pathways. In decarboxylation, oxygen is removed from fatty acids by releasing CO_2 and producing hydrocarbons with one less carbon atom. Meanwhile, decarbonylation eliminates oxygen from fatty acid by forming CO in the presence of hydrogen (Fig. 7). Both routes occur at higher temperatures to allow C–C cleavage.

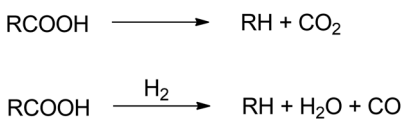

Fig. 7 Decarboxylation and decarbonylation routes.

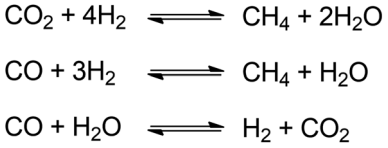

Fig. 8 Methanation and the water gas shift reaction in DCO/DCO_2.

Decarbonylation requires less hydrogen than hydrodeoxygenation, whereas decarboxylation proceeds in the absence of hydrogen.[46,47] The excess of hydrogen initiates methanation or water gas shift reaction, where the CO or CO_2 reacting with hydrogen as described in Fig. 8.[48] Under hydrogen atmosphere, methanation and water gas shift might occur causing the decarboxylation and decarbonylation hardly to be distinguished.

The deoxygenation process has been employed on the production of green diesel from several feedstocks such as natural oils, fatty acids, and FAME (biodiesel). Waste cooking oil was successfully converted to green diesel after two hours. The deoxygenation was conducted at 300 °C and produced heptadecane–octadecane as the main product and several intermediates including fatty alcohols, fatty esters, and fatty acids.[49] Deoxygenation of oleic acid over Pt/P@MIL-101 exhibited 95% yield with 75.5% heptadecane selectivity, conveying the preferable decarboxylation/decarbonylation route.[50] Šimáček and Kubička[51] reported that rapeseed oil was completely converted at 280 °C after one hour reaction. Hexadecane, heptadecane, and octadecane were the main products with fatty alcohols, fatty esters, and fatty acids as the intermediates. Soybean was successfully deoxygenated over $NiMo/Al_2O_3$, Ni/Al_2O_3 and Pd/Al_2O_3.[52] The highest conversion was reported to be 92.9% generated over a bimetallic catalyst $NiMo/Al_2O_3$. Decarboxylation was favoured over Ni/Al_2O_3 and Pd/Al_2O_3 indicated by the high selectivity of heptadecane up to 80%. Srifa *et al.*[53] investigated the catalytic behaviour of Ni/γ-Al_2O_3 and Co/γ-Al_2O_3 on the hydrodeoxygenation of palm oil. Catalysts exhibited excellent performances with more than 90% yield. The selectivity of the product was influenced by the catalysts, where decarboxylation/decarbonylation was favourable over Ni/γ-Al_2O_3 and all routes were dominant over Co/γ-Al_2O_3.

The complicated steps of natural oil deoxygenation has lead many attempts to adopt simpler compound as feedstock such as fatty acid and FAME. A simple fatty acid was mostly applied as model compound to investigate the mechanism of deoxygenation, reaction steps, and some related parameters. In addition, saturated fatty acid was the most attractive model compound that avoid the competition between the hydrogenation of double bond and fatty acid. Since the enthalpy required to break C=C bond (614 kJ mol^{-1}) is lower than a C=O bond (799 kJ mol^{-1}), the hydrogenation of C=C double bond proceeds before deoxygenation,[54] as confirmed by the study of oleic acid and palmitic deoxygenation. Oleic acid deoxygenation attained 92% conversion while palmitic acid was completely transformed at the same reaction condition.[55] Similar result was observed on the deoxygenation of oleic acid over catalyst Ni_2P/Al-SBA-15.[56] Oliveira Camargo *et al.*[56] investigated the deoxygenation of oleic acid over catalyst Ni_2P/Al-SBA-15. Decarbonylation was proposed as the main route with heptadecane as the main product. Pimenta *et al.* claimed that hydrodeoxygenation was two folds more selective in the deoxygenation of stearic acid

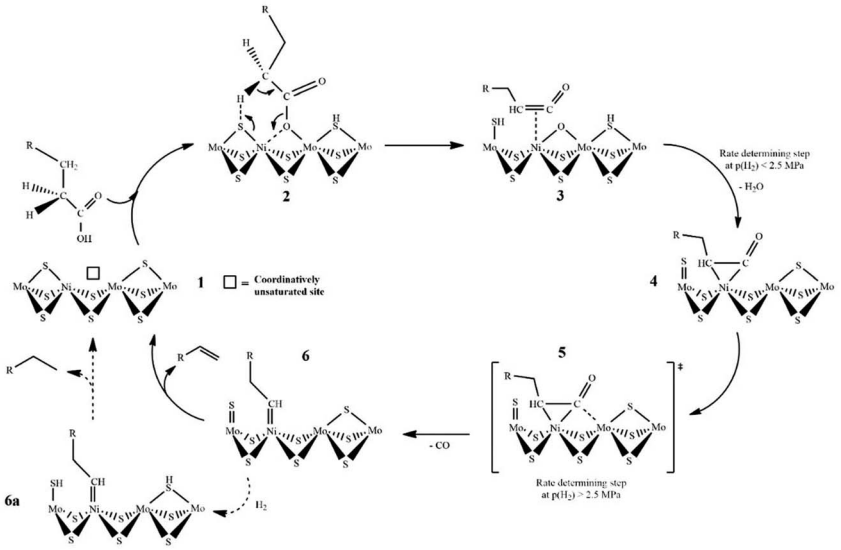

Fig. 9 Proposed mechanism of fatty acid decarbonylation on Ni–MoS_2 catalyst.

over NiMo catalysts. Other catalysts like $NiMo/Al_2O_3$, the selectively favoured decarboxylation.[57]

A reaction mechanism study on fatty acid deoxygenation was reported in many studies. Wagenhofer *et al.* proposed a mechanism for decarbonylation of fatty acids over Ni–MoS_2 catalyst as illustrated in Fig. 9.[58] Partial replacement of Mo with Ni reduced the bonding energy of sulphur atoms, hence increasing the number of sulphur vacancies. These sulfur vacancies and metallic Ni acted as active sites in decarbonylation.

The reduction of sulphur binding energy inclined electron density of neighbouring sulphur, consequently increasing the basicity of sulphur to deprotonate fatty acids. First, fatty acids are adsorbed onto sulphur and Ni to form Ni–O bonds and activated acyl compounds. Afterwards, the C–O bond scission was induced by a strong interaction with the oxophilic Mo cation and the sulphur atom catches the alpha hydrogen to produce the ketene intermediate. This ketene subsequently formed a η^2(C–C) geometry complex. Furthermore, the C–C bond scission on the ketene generated CO gas. Finally, the removal of the substrate on the surface of catalyst generated alkanes or alkene (C_{n-1}).[58]

The mechanism of carboxylic acid decarboxylation was studied on a Pd/C in the form of α-phase palladium hydride (α-PdH_x). The C–H bond of carboxylic acid was cleaved on the surface of Pd creating intermediate R(C_{n-1})–CH*–COO*. Furthermore, the intermediate underwent C–COO bond cleavage resulting in R(C_{n-1})–CH* and reacted with two adsorbed H to produce R(C_{n-1})–CH_3.[59] A similar explanation can be seen in other studies.[60,61]

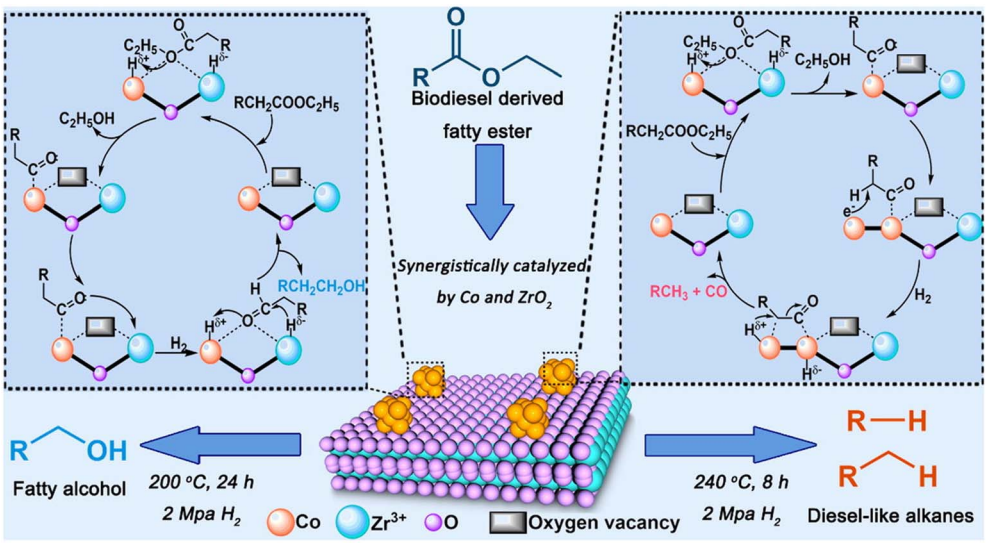

Fig. 10 The influence of catalyst, temperature, and pressure on the reaction mechanism of FAME deoxygenation over Co/ZrO_2. This figure has been adapted from ref. 65 with permission from Elsevier, copyright 2020.

The last promising feedstock is biodiesel or fatty acid methyl ester (FAME). This feedstock is beneficial since biodiesel can be prepared from natural oil through a simple transesterification. Deoxygenation reaction allows the catalytic upgrade of methyl ester with associated fuel properties issues to alkanes. Several studies reported the successful transformation of FAME through deoxygenation. Yang *et al.*[62] tested the activity of the catalyst Ni–ZrO_2 for the deoxygenation of methyl laurate at 280 °C and 2 MPa. Undecane was the main product over dodecane confirming the dominance of decarboxylation/decarbonylation pathway over hydrodeoxygenation. Lauric acid appeared to be the primary intermediate followed by lauryl alcohol. Bie *et al.*[63] investigated deoxygenation of methyl palmitate over catalyst Rh/ZrO_2 at 270 °C and 8 MPa. Decarboxylation/decarbonylation was the major reaction route affirmed by higher selectivity of pentadecane than hexadecane. Several intermediates involved in the process including palmitic acid, hexadecanol, palmityl palmitate and hexadecanal. The deoxygenation of methyl stearate was accomplished using Ru/H-ZSM-5. This catalyst demonstrated high activity with 98.2% conversion after 8 hours reaction at 220 °C. Heptadecane and octadecane were the main product, resulted from several steps including hydrogenolysis and hydrolysis.[64] Methyl palmitate was oxygenated to pentadecane over Ni/Al-SBA-15 catalyst through decarbonylation route, with 66% selectivity at 99.3% conversion.[65]

Regardless of the feedstock, the green diesel production as well as the main reaction pathway are determined by several parameters including temperature, pressure, and catalyst. For instance, the deoxygenation FAME over Co/ZrO_2 where the reaction route and the product were influenced by the catalyst, reaction temperature and pressure (Fig. 10).[66]

6. Influence of temperature

Reaction temperature significantly effects the green diesel production. In general, deoxygenation reaction proceeds at the temperature range of 200–400 °C. Higher temperature is not advisable due to the possibility of alkane cracking that result many compounds in various range leading to the lower selectivity of desired alkanes. In addition, catalysts mostly proned to deactivation due to coke formation, carbon deposition and sintering at high temperature. The collapsed structure due to an elevated temperature also lowered the catalytic activity.[67,68] The increase of temperature improves conversion or yield of green diesel. The optimum yield of tall oil fatty acid deoxygenation was obtained at 350 °C.[69,70] Altering the temperature from 260 °C to 300 °C permitted the completely converted of methyl stearate from initial conversion of 65%.[71] The incline of conversion from 52% to 89% was also occurred on the deoxygenation of oleic acid when the temperature rose from 300 to 350 °C.[72] The optimum yield of palm oil deoxygenation was obtained at 375 °C.[67] Šimáček *et al.*[70] declared that conversion of rapeseed oil increased with the raise of temperature where all reactants as well as intermediates were completely transformed at 310 °C. Similar result were also observed elsewhere.[11,73–80]

Apart from conversion, reaction temperature also determines the reaction pathway assigned by the selectivity of the products. Higher temperature favours decarboxylation/decarbonylation since this condition allow C–C cleavage and carboxylic group release as CO_2 or CO. The optimum temperature to break the carboxylic group was 375 °C.[81]

The influence of reaction temperature on the reaction route was mentioned in many studies. At an elevating temperature of 260 °C to 300 °C on the deoxygenation of methyl stearate over CoNi/HAP, the selectivity of heptadecane inclined, followed by the decline of octadecanol selectivity indicating the occurrence of DCO/DCO_2.[71] Deoxygenation of rapeseed oil at a span temperature of 260–340 °C affirmed that higher temperature favoured decarboxylation indicated by low C_{18}/C_{17} ratio.[82] Moreover, deoxygenation of palmitic acid produced CO_2 as indicator of decarboxylation presented at above 290 °C.[83] A similar result was obtained from numerous studies.[70,84–87]

Some studies suggested that the high temperature was not applicable due to sintering phenomenon. To address this issue, HZSM-5 was opted to hinder the movement of metal particles at high temperature.[88] Another study proposed ionic liquid as coating material to stabilize single atom catalyst such as Pd_1/HAP. Ionic liquid covered the metal atom increased the kinetic barrier for the formation of metal–metal bond on the catalyst surface. In addition, the presence of ionic liquid caused the formation of metal aggregates become thermodynamically less favorable.[89]

7. Influence of pressure

The presence of hydrogen is critical for deoxygenation, especially, oxygen removal and catalytic activity maintenance.[90] Overall, green diesel production occurs at hydrogen pressure within the range of 1–10 MPa.[17]

Comparable to reaction temperature, hydrogen pressure also has a significant role in both reaction results and pathways. In terms of oil feedstock, hydrogen is urgently required to transform triglycerides into fatty acids. Higher pressures of hydrogen generates higher conversions as reported in the deoxygenation of soybean oil, palmitic acid, and other feedstocks.[69,91,92]

Oleic acid was 55.5% converted over Ni–Fe/ZrO_2 at 1 MPa and 97.98% at 3 MPa.[93] Raising the hydrogen pressure from 0.7 to 3 MPa improved the stearic conversion from 53% to 99% at deoxygenation of stearic acid over Ni–γ-Al_2O_3 catalyst.[94] Notably, high pressure provided sufficient hydrogen to completely transform the feedstock.[95] The enhanced conversion due to hydrogen pressure can be observed in other studies.[67,96–98]

Aside from conversion, hydrogen pressure also regulates the reaction pathway. Under rich hydrogen environment, hydrodeoxygenation takes place predominantly.[25,99,100] Low hydrogen availability encouraged decarbonylation route, however the presence of hydrogen unnecessarily required in the decarboxylation.

The influence of hydrogen pressure on the reaction pathway was confirmed in the deoxygenation of methyl palmitate over Co_3Mo_3N catalyst. Within the range of hydrogen pressure 1–4 MPa, the hydrodeoxygenation progressed as inferred by the improvement of hexadecane selectivity from 54% to 97%.[101] The

ratio of C_{18}/C_{17} in the deoxygenation of rapeseed oil inclined with the rise of hydrogen pressure.[100] Furthermore, higher hydrogen pressure inhibited decarboxylation in the decarboxylation of free fatty acids over 5 wt% Pd/C at 300 °C under 5% H_2.[99] The reaction pathway shifted from decarboxylation to decarbonylation was proven by the transformation of CO_2 to CO with the increase of hydrogen pressure.

Contrary, the pentadecane was the main product in deoxygenation of methyl palmitate over B_2O_3/ZrO_2 even when the hydrogen pressure was varied between 2-8 MPa.[29] Similar result was observed in the deoxygenation of stearic acid over Ni/γ-Al_2O_3. Heptadecane selectivity shifted from 49% to 96% when the pressure increased.[102] Furthermore, HDO pathway produces intermediates like aldehydes that enable DCO pathway to take over. These contradictive results underlined the other factor influencing the reaction route, especially the catalyst.

8. Influence of reaction time

Reaction time is the most common and unemphasized parameter in green diesel production. This parameter is automatically investigated in every study which the general result inferred that conversion inclined as the function of reaction time.[103] Prolonged reaction time provided adequate interaction between reactant and catalyst. The value of reaction time is varied from 30 minutes to 48 hours and slightly beyond.[104] Notably, the maximum reaction differed depends upon the other reaction condition such as feedstock, catalyst, reaction temperature and pressure.[105]

The explicit reaction time influence was investigated on deoxygenation of waste cooking oil and its derivatives over NiCo/SBA-15.[11] Within 2 hours, the product yield increased from 18% to 80% and hydrocarbon selectivity inclined from 31% to 70%. The study on methyl laurate over Co/ZSM-5 reported similar trend with the maximum conversion was attained after 4 hours.[106]

Nevertheless, excessive extended reaction time was inadvisable in regards to product selectivity. The products underwent side reactions such as cracking, isomerisation, cyclization, and dimerization in prolonged reaction time leading to low hydrocarbon selectivity.[67,107]

In the matter of reaction pathway, the influence of reaction time was reported negligible below the maximum region. The deoxygenation of oleic acid over Ni/MgO–Al_2O_3 claimed the raising conversion and hydrocarbon yield without any change on the selectivity profile. Octadecane was produced in a rapid rate compared to heptadecane affirming HDO as the min pathway. The shift of pathway was not observed within 3 hours of reaction.[108]

9. Influence of catalyst

Catalyst is the most important factor in the deoxygenation of vegetable oil and its derivatives. Supported metal catalysts are the most applied catalysts in most research. Several properties

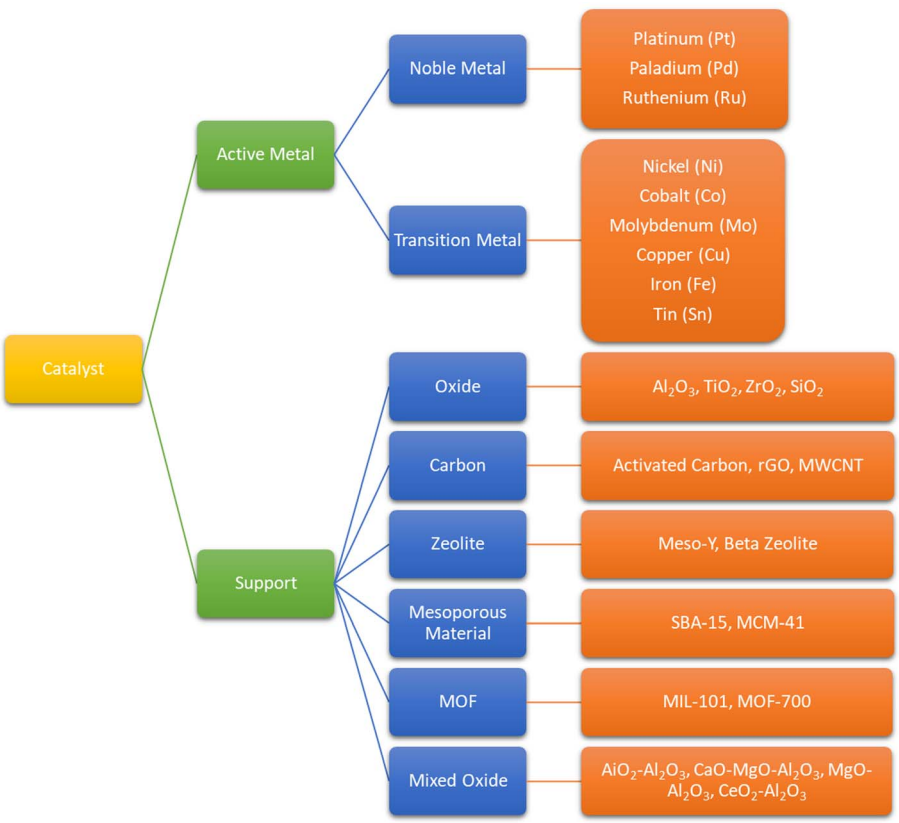

Fig. 11 Active metal and support material commonly used in biojet production.

of catalyst are crucial for deoxygenation with the purpose of promoting hydrogenation and C–C cleavage, such as high acidity, small particle size with high metal area, excellent dispersion, superior thermal stability.[46,109,110] In terms of hydrodeoxygenation, the ability to split H_2 is inevitable for the catalyst. These beneficial characteristics are associated with the active metal site, metal concentration, catalyst amount and catalyst support. Hence, the employ of metal and support individually define the conversion as well as product selectivity. Fig. 11 explains the active metal and support material employed on deoxygenation of natural oil and its derivatives.

9.1. Effect of metal

In supported metal catalyst, metal performs as the active site accommodating the hydrogen split, hydrogen insertion and C–C cleavage. Metal active sites determine the deoxygenation pathway (HDO, DCO, and DCO_2). In general, metal species in catalysts is classified into noble metals and transition metals. Transition noble metals like platinum (Pt), palladium (Pd), and ruthenium (Ru) are the main metals extensively applied owing to their excellent performance in activity and product selectivity. Nevertheless, these metals demonstrated several issues including expensive cost, water poisoning, deactivation, and dependence on the support which driving these catalysts became less preferable.[45,109,111] Alternatively, nickel (Ni), cobalt (Co) and molybdenum (Mo) were opted as the promising alternative.[52,81,110–113] Pd@PPN catalyst performed a high activity on the deoxygenation of stearic acid with 90% conversion and 83% C_{17} selectivity. The study claimed that the excellent result was attributed to the electron rich palladium (Pd) that activated the interface bound H_2. Another advantage of Pd was robustness to high temperature as claimed in the study of waste cooking oil deoxygenation at 400 °C. However, the maximum desired alkane selectivity only achieved 77% because the alkane underwent cracking process.[114] Comparable result was observed in the activity of platinum (Pt) as deoxygenation catalyst. Generally, Pt catalyst converted about 90% feedstock with 60% main product selectivity.[9,115–117] Excluding the hydrogen pressure, Pd and Pt drive the reaction pathway towards DCO/DCO_2.

Noble metal likes ruthenium (Ru) exhibits highest activity compared to Pt and Pd. Ru/C catalyst activated with $ZnCl_2$ gave 100% conversion of stearic acid at low temperature (140 °C). The selectivity for C_{17} is 88% and C_{18} is 12%, indicating the DCO/DCO_2 pathway is preferable to HDO.[118]

Another study used Ru/TiO_2 for the conversion of ethyl stearate under moderate temperature of 220 °C. Ru/TiO_2 catalyst performed 98.4% conversion with selectivity of C_{17} and C_{18} were 63.8% and 29.5%, respectively.[119] These results indicated the high activity of Ru and its selectivity for the DCO/DCO_2 pathway. Higher activity of Ru compared to Pt and Pd was supported by the high specific rate and turnover frequency (TOF) of the Ru catalyst followed by Pt and Pd. In addition, the surface acid–base characteristics greatly affected the Pt and Pd catalysts, where the presence of phosphate on the carbon support severely reduced the activity of DCO and DCO_2. However, this phenomenon was hardly observed during the employ of Ru catalyst, confirming its superiority in the conversion of fatty acids.[115]

The high price of noble metal catalysts promoted many attempts to pursuit the cheaper and abundant materials such as transition metals. Study on the drubber seed oil deoxygenation claimed that Mo/γ-Al_2O_3 was capable to convert 95% of the oil. Combination of Mo^{6+} and Mo^{4+} active sites directed the reaction pathway toward hydrodeoxygenation with 47% contribution. It is worth noted that the addition of molybdenum (Mo) loading inclined the HDO selectivity.[8] Other results confirmed the application of Mo within conversion in the range of 54–98% with various preference on HDO and/or DCO/DCO_2.[120–122]

Nickel (Ni) and cobalt (Co) were reported as the most promising catalyst since these transition metals embodied excellent properties for deoxygenation reaction. A high conversion of 96.7% was attained from deoxygenation of oleic acid over Ni/MgO–Al_2O_3 at 300 °C and 2 MPa. The metal active site together with the acid site available on support engineered the reaction pathway towards HDO with C_{18} and C_{16} selectivity of 45.9%. The interface of Ni and support provided hydride and protons for reactants. Apart from that, the active site of Ni metal accommodated the hydrogen split and C–C cleavage.[108] Interestingly, Ni also directed the reaction route to DCO/DCO_2 in the deoxygenation of stearic acid at 250 °C and 3 MPa. It was claimed that metal area of Ni was responsible for the high heptadecane selectivity of 90%. Many similar results concluded that Ni catalyst favoured DCO/DCO_2 pathway.[8,116,128,130,132]

In contrast, cobalt catalyst was infamous for proportionally navigating the deoxygenation towards all routes. The Co/ZrO_2 successfully transformed ethyl palmitate to hexadecane and pentadecane at 240 °C and 2 MPa. DCO/DCO_2 pathway was dominant referred by pentadecane selectivity of 54.3%.[66] The cobalt in the form of Co_3O_4/SiO_2–Al_2O_3 catalyzed methyl stearate at 250 °C and 3 MPa. The highest octadecane selectivity of 88% represented the HDO as the major pathway. High dispersion was claimed as the most influencing properties where Co_3O_4 undertook *in situ* reduction to metallic cobalt.[134] The essential role of cobalt in conversion and reaction pathway can also be found elsewhere.[85,106,129,135]

In the quest of the promising transition metal catalyst, some metals have been attempted to provide high conversion with a compromising cost such as copper (Cu), ferum (Fe) and stannum (Sn). Monometallic Cu converted 96% oleic acid at 330 °C and 1 MPa N_2 for 3 hours with tetralin as hydrogen source, where this result was claimed higher over monometallic nickel with 82% conversion at the same reaction conditions. This is because Cu has a better hydrogen liberation ability than Ni as seen from Cu ability to convert tetralin (47%) which is better than Ni (33%).[43]

The high catalytic activity of monometallic Cu was also reported in the production of green diesel from stearic acid.[136] Supported by quantum-chemical simulation, DCO was claimed as the major pathway due to the lower activation energy where DCO_2 required 77.0 kJ mol^{-1} while DCO within the gap of 61.5 kJ mol^{-1}.[137] Improvement on catalytic activity of Cu was attempted by the addition of CeO_2 as promotor. Stearic acid was converted to 96.37% product with alkane selectivity of 88.79%.

The presence of CeO_2 initiate the oxygen vacancies on the surface of Cu permitting the two oxygens of carboxylic functional group to attach on the surface of Cu.[105] Similar results were also observed elsewhere.[138,139]

The application of Fe was also aimed as a cost-effective catalyst in which the Fe^{3+} was expected to promote DCO_2 pathway *via* the formation of Fe^{3+} complex with COO^- as ligands.[142] The Fe/HMS was tested on triolein deoxygenation at 380 °C for 2 hours. This reaction generated 81.4% conversion and 96.4% C_8–C_{18} selectivity with DCO/DCO_2 as the favourable route. This result was claimed as the result of excellent dispersion of Fe and the synergistic interaction of Fe–SiO bonds. Newly formed Fe–SiO bond created new acid site, thus increase the amount of weak-medium acid site leading to the high conversion and selectivity.[140]

In a contrast, lower alkane selectivity of 52% was reported on the deoxygenation of palmitic acid over Fe/AC at 450 °C for 30 minutes with hydrocarbon yield of 55%.[141] A slightly higher alkane selectivity of 60.7% was also found in the palmitic acid over Fe_2O_3/Al-MCM-41.[142] Despite the excellent alkane selectivity, the employ of Fe catalyst generated lower conversion compared to other catalyst such as nickel. The conversion remained within the range of 75–89%.[143,144]

Those phenomena commenced the idea of Ni application alongside with Fe as bimetallic catalyst. The Ni–Fe/ZrO_2 catalyst elevated the conversion of oleic acid up to 98.7% over the following reaction conditions: 240 °C, 2 MPa and 3 hours.[93] In terms of selectivity, the existence of Fe assisted the reaction pathway owing to the oxophilic Fe that particularly adsorbed and activated the carboxylic acid towards DCO/DCO_2.[145] Nevertheless, Fe behaved as promotor to Ni and assisted the reduction time by lowering the NiO reduction temperature leading to the smaller particle size and higher surface area.[93] Similar results can be seen in other studies.[48,146,147]

Another less applicable metal in deoxygenation is Sn which commonly used in the form of bimetal catalyst. The sole Sn metal displayed low to moderate conversion and selectivity causing the role of Sn as the promotor metal. For instance, deoxygenation of rapeseed oil over Pt–Sn/Al_2O_3 achieved 87.37% conversion and promoted the HDO pathway.[148,154,155] In monometallic Pt, two oxygen atoms of fatty acid formed a chelate with Pt on catalyst surface and underwent hydrogenolysis to produce aldehyde. Afterwards, the aldehyde undertook C–C scission and CO was released. The addition of Sn hindered the decarbonylation by adsorbing the oxygen atom of aldehyde carbonyl group permitting further hydrogenation to occur.[149] This pathway was supported by the high activity of Pt in hydrogen split. Under a rich hydrogen environment, the aldehyde was transformed to alcohol and then alkanes. Moreover, Sn was also in charge of lowering the reduction temperature producing Pt with smaller particle size and improved surface area, as exhibited in the Pt–Sn/SAPO-11.[150] Furthermore, the presence of Sn also increased the Lewis acid sites that enhanced the catalytic activity. Other studies can be found elsewhere.[151–153]

In general, the noble metal catalyst performed high activity at relatively lower temperature and effectively drove the pathway towards DCO/DCO_2 in the absence of hydrogen. At rich hydrogen environment, noble metal catalysts favoured HDO route. On the other hand, transition metal required high temperature and depended on the associated reaction condition to engineer the reaction pathway. Table 2 summarizes the influence of catalyst and reaction condition of deoxygenation of various feedstocks.

As far, metal concentration and dispersion were highlighted as the main effecting properties followed by the acidity of the support. The increase of Ni loading from 1 wt% to 15 wt% generated higher conversion of FAME from 24.8% to 89.3%.[156] The effect of metal loading was also confirmed by Miao *et al.*[83] Higher conversion of palmitic acid was obtained with the increase of metal loading from 0 wt% to 20 wt%. Conversion of soybean oil over Ni/Al_2O_3 sharply inclined from 60.8% to 95.9% by the addition of catalyst amount.[52] Kwon *et al.* investigated the impact of catalyst amount in deoxygenation of canola oil over NiMo/γ-Al_2O_3 within the catalyst mass range of 0.026–0.102 g.[157] The result described that heptadecane and octadecane simultaneously increased as a function of the catalyst amount.[157]

Another influential factor of catalyst was the catalyst support that steer the reaction leaning towards particular pathway as described in the following section.

9.2. Effect of support

Catalyst support embodies excellent criteria in terms of porosity, metal–support interaction, acidity and thermal acidity. The nature of porosity supplies fundamental characteristic of heterogeneous catalyst including surface area, pore size and pore volume.[46,109] These characteristics address the availability of the internal surface to accommodate the active sites, and the accessibility of reactant toward active sites.[158] Thermal stability was high necessity since the impregnation method involves calcination and deoxygenation process carried out at elevated temperature. The other catalyst support characteristics display the important function to direct the reaction pathway in green diesel production.

Pore size was claimed as the main property of the Ni/zeolite Y on the deoxygenation of microalgae biodiesel. The large pore size of zeolite Y (3.9 nm) prevented mass transfer limitation since methyl palmitate molecule size was smaller (2.5 nm). Expectedly, high conversion of 91.5% was attained at 275 °C and 2 MPa.[159] The critical function of pore size was also implied by the deoxygenation of triglycerides over beta zeolite supported catalysts. Low conversion was reported as the result of pore accessibility issues as beta zeolite pore diameter was 5.7 nm while triglyceride size was 7.5 nm.[160]

Apart from the porosity, acidity of zeolite also plays significant role as elaborated in the deoxygenation of palm fatty acid with 84.8% conversion and 78.2% selectivity of $C_{15–17}$. The acidity of zeolite that influenced by the Si/Al, addressed the availability of Lewis and Brønsted acid sites.[161] The addition of metal into zeolite replaced the proton through an ion exchange, lowering number of Brønsted acid sites and increasing Lewis acid sites.[47] Lowered Brønsted acid sites inhibited the cracking and coking process.

Table 2 Studies on the biojet production using noble and transition metal catalysts

Catalysts	Feedstock	Condition	Conv. (%)	Selectivity	Ref.
Pd@PPN	Stearic acid	150 °C, 2 MPa H_2, 14 h, batch reactor	90	C_{17} = 83%	123
Pd/SBA-15	Stearic acid	300 °C, 1.7 MPa 5% H_2, 5 h, semi batch reactor	96	C_{17} = 98%	124
Pd/C	Waste cooking oil	400 °C, no H_2, 2 h, batch reactor	100	*n*-Paraffin = 71%	114
Pd/C	Stearic acid	300 °C, 1.7 MPa 5% H_2, 3 h, semi batch reactor	94	C_{17} = 99%	110
Pd/C	Stearic acid	300 °C, 1.5 MPa 10% H_2, 0.5 h, batch reactor	100	C_{17} = 98%	125
Pd/C	Stearic acid	300 °C, 1.5 MPa 5% H_2, 3 h, batch reactor	95	C_{17} = 99%	99
Pd/C	Lauric acid	300 °C, 2 MPa H_2, 5 h, semi batch reactor	70	C_{11} = 90%	126
Pd/C	Tall oil fatty acid	300 °C, 1.7 MPa 1% H_2, 3 h, batch reactor	90	C_{17} = 95%	69
Pd/C	Castor oil	340 °C, 2.5 MPa H_2, 7 h, batch reactor	95	C_{17} = 87% C_{18} = 9%	127
Pd/AC	Tristearin	326 °C, 3 h, batch reactor	100	C_{17} = 54%	115
Pd	Soybean oil	400 °C, 9.2 MPa H_2, 2 h, batch reactor	91	C_{17} = 96%	128
Pd/Al_2O_3	Palm oil	330 °C, 4 MPa H_2, flow reactor	100	C_{17} = 79.5% C_{18} = 4.7%	129
Pt/AC	Tristearin	326 °C, 3 h, batch reactor	100	C_{17} = 64%	115
Pt/Al_2O_3	Palm oil	330 °C, 4 MPa H_2, flow reactor	100	C_{17} = 72% C_{18} = 7.6%	129
Pt/Al_2O_3	Tristearin	260 °C, 4 MPa H_2, 3 h, semi batch reactor	5	C_{17} = 65%	116
Pt/θ-Al_2O_3	Soybean oil	360 °C, 5 MPa H_2, 2 h, fixed bed reactor	81	$C_{13,15,17}$ = 63%	117
Pt/C	Crude palm kernel oil	420 °C, 3.5 MPa H_2, 10 h, fixed bed reactor	59	C_{8-16} = 28%	9
Ru/C	Stearic acid	140 °C, 5 MPa H_2, 6 h, batch reactor	100	C_{17} = 88% C_{18} = 12%	118
Ru/C	Corn stover oil	3000 °C, 12.5 MPa H_2, 4 h, batch reactor	66	—	84
Ru/TiO_2	Ethyl stearate	220 °C, 10 MPa H_2, 6 h, batch reactor	98	C_{17} = 64% C_{18} = 30%	119
Mo/γ-Al_2O_3	Rubber seed oil	350.15 °C, 3.5 MPa H_2, 3 h, fixed bed reactor	95	C_{17} = 20% C_{18} = 32%	8
Mo/Al_2O_3	Rapeseed oil	270 °C, 3.5 MPa H_2, 4 h, fixed bed reactor	100	C_{18} = 90%	100
Mo/AC	Palm fatty acid distillate	350 °C, no H_2, 1 h, batch reactor	54	C_{15+17} = 45%	120
Pt–MoO_x/ZrO_2	Oleic acid	220 °C, 2 MPa H_2, 5 h, batch reactor	94	C_{17} = 14% C_{18} = 63%	121
MoS_2/γ-Al_2O_3	Oleic acid	400 °C, 4 MPa H_2, 3 h, batch reactor	97.91	C_{17} = 65% C_{18} = 35%	122
Ni/CeO_2–Al_2O_3	Methyl laurate	300 °C, 3 MPa 10% H_2/N_2, 4 h, semi batch reactor	100	C_{11} = 99% C_{12} = 2%	130
Ni/Al_2O_3	Tristearin	260 °C, 4 MPa H_2, 3 h, semi batch reactor	2	C_{17} = 83%	116
Ni/Al_2O_3	Palm oil	330 °C, 4 MPa H_2, flow reactor	100	C_{17} = 80% C_{18} = 2%	129
Ni/γ-Al_2O_3	Rubber seed oil	350.15 °C, 3.5 MPa H_2, 3 h, fixed bed reactor	95	C_{17} = 22% C_{18} = 5% C_{15} = 23%	8
Ni/MgO–Al_2O_3	Oleic acid	300 °C, 2 MPa H_2, 3 h, batch reactor	96.7	C_{16-18} = 46%	108
NiMo/Al_2O_3	Rapeseed oil	260 °C, 7 MPa H_2, 2 h, flow reactor	—	C_{18} = 39.6% C_{17} = 4.7%	70
NiMoC/Al-SBA-15	Soybean oil	400 °C, 4.5 MPa H_2, 2 d, fixed bed reactor	96	C_{15-18} = 97%	131
Ni/HPS	Stearic acid	250 °C, 3 MPa N_2, 1 h, fixed bed reactor	100	C_{17} = 90%	132
Co/ZrO_2	Ethyl palmitate	240 °C, 2 MPa H_2, 8 h, batch reactor	100	C_{15} = 54% C_{16} = 12%	133
Co/Al_2O_3	Palm oil	330 °C, 4 MPa H_2, flow reactor	100	C_{17} = 34% C_{18} = 50%	129
Co_3O_4/SiO_2–Al_2O_3	Methyl stearate	250 °C, 3 MPa H_2, 6 h, batch reactor	100	C_{17} = 10% C_{18} = 88%	134
CoMo/Al_2O_3	Rapeseed oil	270 °C, 5 MPa H_2, batch reactor	100	C_{18}/C_{17} = 20	85
Co@SiO_2	Palmitic acid	300 °C, 2 MPa H_2, 4 h, batch reactor	100	C_{16} = 71%	135
Co-MOF-700	Methyl laurate	280 °C, 2 MPa H_2, 4 h, batch reactor	100	C_{11} = 68% C_{12} = 18%	106
Cu	Oleic acid	330 °C, 1 MPa N_2, 3 h, batch reactor	96	C_{17} = 28%	43
Cu/γ-Al_2O_3	Stearic acid	350 °C, 1.4 MPa H_2, 6 h, batch reactor	95,5	C_{17} = 78%	136
Cu/γ-Al_2O_3	Stearic acid	350 °C, 1.4 MPa H_2, 1 h, batch reactor	45	C_{17} = 67%	137

Table 2 (*Contd.*)

Catalysts	Feedstock	Condition	Conv. (%)	Selectivity	Ref.
$CuO–CeO_2/\gamma\text{-}Al_2O_3$	Stearic acid	300 °C, 4 MPa H_2, 12 h, batch reactor	96	—	105
CuCo/CNT	Stearic acid	260 °C, 3 MPa H_2, 4 h, batch reactor	100	C_{17} = 88% C_{18} = 6%	138
$Cu–Ni/ZrO_2$	Oleic acid	350 °C, 3 h, batch reactor	100	C_{17} = 67%	139
Fe/HMS	Triolein	380 °C, 2 h, batch reactor	82	$C_{8–18}$ = 97%	140
Fe/AC	Waste cooking oil	450 °C, 0.5 h, fixed bed reactor	94	C_{15+17} = 52%	141
Fe_2O_3/Al-MCM-41	Palmitic acid	350 °C, 2 h, batch reactor	77	C_{15} = 61%	142
CFeAl	Oleic acid	300 °C, 3 h, batch reactor	89	$C_{13–20}$ = 77%	143
Fe/CMD900	Waste cooking oil	390 °C, 0.5 h, batch reactor	55	$C_{13–20}$ = 38%	144
$Ni–Fe/ZrO_2$	Oleic acid	240 °C, 2 MPa H_2, 3 h, batch reactor	99	—	93
FeNi/C	Stearic acid	330 °C, 3 h, batch reactor	100	C_{17} = 77%	145
$NiO–Fe_2O_3$/MWCNT	*Jatropha curcas* oil	350 °C, 1 h, semi-batch reactor	73	C_{15+17} = 63%	48
$Ni–Fe/Al_2O_3$	Waste cooking oil	375 °C, 24 h, fixed bed reactor	100	$C_{10–20}$ = 95%	146
Ni–Fe/SBA-15	Waste cooking oil	350 °C, 2 h, semi batch reactor	73	$C_{15–17}$ = 41%	147
$Pt–Sn/Al_2O_3$	Rapeseed oil	400 °C, fixed bed reactor	100	C_{18} = 84%	148
PtSn/SAPO-11	Methyl palmitate	375 °C, 3 MPa H_2, 3 h, fixed bed reactor	87	C_{15+16} = 79%	149
Pt–Sn/SAPO-11	Waste lard oil	380 °C, 5 MPa H_2, fixed bed reactor	97	$C_{15–18}$ = 65%	150
$Pt–Sn/Al_2O_3$	Rapeseed oil	400 °C, 5 MPa H_2, fixed bed reactor	100	C_{18} = 84%	151
Ni–Sn/C	Methyl palmitate	330 °C, 1 MPa N_2, 6 h, batch reactor	99	C_{15} = 88% C_{16} = 5%	152
$Ni–Sn/Al_2O_3$	Tristearin	350 °C, 4 MPa N_2, 6 h, semi batch reactor	99	C_{17} = 55%	153

Brønsted acid site enabled proton mobility and improved the contact between the external acid site with metal particle that leads to the DCO/DCO_2 pathway.[162] On the other hand, Lewis acid sites activated carboxylate and carbonyl group, promoting HDO route.[134] Other studies claimed zeolite acid sites improved metal dispersion and metal–support interaction.[163]

The second common catalyst support is Al_2O_3 which associated with metal–support interaction properties and metal dispersion. Higher dispersion provides more active site exposed on the surface of catalyst. Al_2O_3 support inclined the dispersion of Ni–Mo–S metal on the $NiMoS_2/Al_2O_3$ catalyst leading to high conversion and hydrocarbon yield on the deoxygenation of palm oil at 300 °C and 4 MPa.[164]

Profound study of Al_2O_3 crystal structure on Pt dispersion in the deoxygenation of triglyceride had been carried out by Oh *et al.* Gamma and beta alumina displayed the highest Pt dispersion due to the availability of pentacoordinate site. In terms of catalytic activity $Pt/\gamma\text{-}Al_2O_3$ displayed highest paraffin yield of 78% at higher conversion due to the larger pore size over $\theta\text{-}Al_2O_3$.[117] In case of Ni/Al_2O_3, the strong Ni interaction with Al_2O_3 created $NiAl_2O_4$, a new active site as DCO/DCO_2 driving force.[165]

The next common catalyst support is SiO_2 which is less acidic compared to Al_2O_3. Many studies reported the employ of SiO_2 support combined with various metals. Deoxygenation of oleic acid over $Co_xNi_{1-x}P/SiO_2$ at 320 °C and 2 MPa generated 98% conversion and 86% heptadecane selectivity.[166] The favored DCO/DCO_2 pathway was also found in the deoxygenation of palmitic acid over Co/SiO_2 at 260 °C and 2 MPa with 51.9% C_{15} selectivity. This high result was due to the high surface area (315 $m^2\ g^{-1}$) and large pore diameter (36 nm). Notably, the acidity level of this catalyst was very low (0.01 mmol NH_3 per g) that susceptible for further hydrogenation to occur.[167] Other studies also mentioned the application of SiO_2 as catalyst support.[135]

Other studies attempt to combine Al_2O_3 and SiO_2. An improvement in terms of conversion and selectivity was reported in the deoxygenation of tristearin over $Ni–Pd/Al_2O_3–SiO_2$. About 99.5% tristearin was achieved over this following reaction conditions: 260 °C, 4 MPa for 3 hours. The application of this catalyst shifted the reaction pathway towards HDO from 0% to 31% selectivity of C_{18}.[168]

Another support mentioned in the literature is ZrO_2. For the sake of comparison, Papageridis *et al.*, investigated the influence of catalyst supports (Al_2O_3, SiO_2, ZrO_2) on palm oil conversion. The Ni/ZrO_2 exhibited the highest dispersion and more abundance of acid sites. This superior characteristic rendered the ZrO_2 as the most effective support in the lowest optimal temperature.[169] Furthermore, ZrO_2 support provided oxygen vacancies acting as active site for ethyl palmitate adsorption, activating the carbonyl groups and stabilizing intermediates.[66]

The same phenomenon was also observed in TiO_2 support as proposed in the mechanism of deoxygenation over Pd/TiO_2. Nanoparticle Pd facilitated H_2 dissociation where the hydrogen was able to migrate TiO_2 and induced the reduction of Ti^{4+} to Ti^{3+}. This hydrogen spill over caused some defect in TiO_2 structure and oxygen vacancy was formed. The reduction induced the feasible movement of electron from reduced TiO_2 to Pd. Subsequently, electron rich Pd effectively activate oxygen in carboxylic/carbonyl group. In addition, the defects on TiO_2 provide anchorage sites for Pd particles thereby preventing particle size growth, leading to higher Pd dispersion.[170] In spite of high selectivity, the conversion generated from deoxygenation metal supported TiO_2 was still below the common support such as Al_2O_3, SiO_2 and zeolite. The $WO_3/Pt/TiO_2$ transformed

86% of jatropha fatty acids at 410 °C and 4 MPa (10% H_2), with the C_{15+17} selectivity of 65%.[171] The use of TiO_2 as catalyst support was also mentioned in other studies.[28,172]

In respect of surface area, activated carbon attracted many attempts to be applied in deoxygenation reaction. For instance, Ni/AC contain surface area of 584 $m^2\ g^{-1}$ with acid sites of 19 120 μmol g^{-1}. This trait was in charge of C–O activation and C–C cleavage. Moreover, Ni/AC possessed low to moderate basic sites of 4960 μmol g^{-1}, enhancing the C–O scission in DCO pathway. This characteristic enable to convert 90% of waste cooking oil to 89% of C_{15} and C_{17}, indicating the DCO/DCO_2 route. Although Ni catalyst was commonly prone to deactivation due to coke formation, the high surface area of activated carbon contain sufficient space for adsorption of hydrocarbons formed during deoxygenation.[173] The role of basic sites on directing the reaction route was also investigated in the conversion of chicken fat oil over Ni–Mn/MWCNT. The CO_2 production inclined as the function of the number of basic sites. The preferable decarboxylation route was acclaimed by the selectivity of C_{15+17} up to 83%.[174] Contrary, very low conversion of 6% was resulted from deoxygenation of methyl laurate over Co/C due to the high strength adsorption capacity of C, making it hardly released the products.[106] This was the reason activated carbon rarely used as support material in deoxygenation. Similar result can be seen in other studies.[175,176]

10. Future outlook

Paris Agreement that set a goal to limit the global emissions to zero and temperature increases to 1.5 °C by 2050, reflects a heightened level of concern about the negative effects of climate change.[177] This ultimate goal can be achieved by focusing on the elevation of the existing solutions involving six technological avenues to reach 36.9 giga tonnes CO_2 emission cut off (Fig. 12).[178] Renewable energy was positioned in the same level priority as electricity efficiency with renewable sustainable biomass as the primary driver.[178] In addition, rapid decarbonising has been achieved through the electricity efficiency as well as electrification generated from green resource involving solar, wind and hydro. However, long distance transport particularly aviation remained as challenging issue and takes decade away

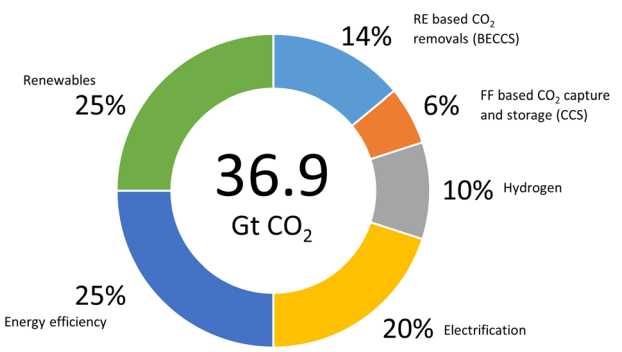

Fig. 12 Reducing emissions by 2050 through six technological avenues (redraw from ref. 177)

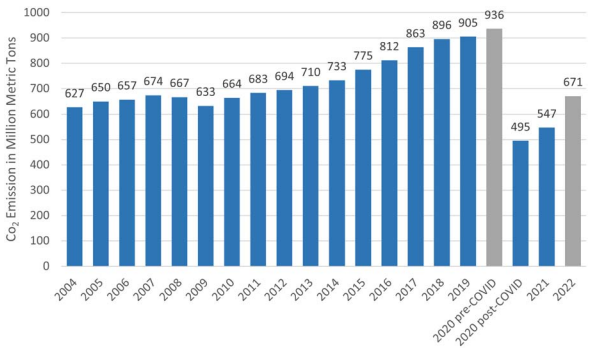

Fig. 13 Carbon dioxide emissions from commercial aviation worldwide from 2004 to 2022 (https://www.statista.com/statistics/1186820/co2-emissions-commercial-aviation-worldwide).

to commercialise.[5] This matter has urged many attempts to fine the solution since aviation sector contributed on 2% of global CO_2 emission and about 671 metric tonnes in 2022 (Fig. 13).[177] Therefore, the application of biojet/sustainable aviation fuel is beneficial.

The current development of sustainable aviation fuel has been reported by The International Civil Aviation Organization by 2022. About 350 000 commercial flights have used biojet fuel which distributed in 45 airports. About 21.6 billion liters of SAF is under offtake agreements and 9 conversion processes has been certified. Moreover, 22 policies associated to sustainable aviation fuel has been adopted or under development.[179] Nevertheless, ongoing improvement seems hardly achieve the net zero target and the acceleration is urgently required.[178] In consequence, the biojet demand will rapidly increase for the following future.

On a net zero trajectory, biofuel demand is estimated to reach 14 EJ in 2040 and acceleration up to 30% in 2027.[180] In more detail, the demand of biodiesel together with biojet fuel is estimated to incline by 44% or 21 billion litres in the span of 2022–2027 (Fig. 14). This consumption growth is the result of increasing demand in major countries such as The United States, Europe, Brazil and Indonesia. In United State, the biofuel requirement is fulfilled by the domestic production using various feedstocks including soybean oil, rapeseed oil, corn oil, used cooking oil and animal fats. The most increasing demand

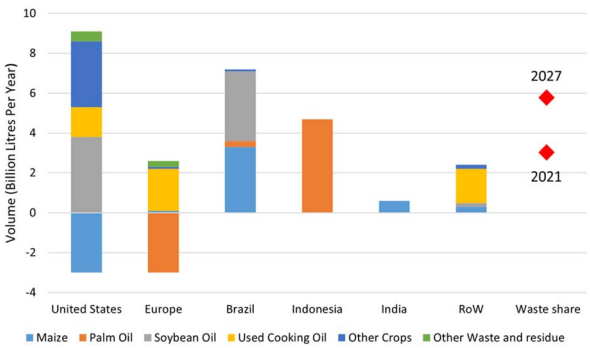

Fig. 14 Total biofuel growth from 2021 to 2027 (estimation).[179]

of renewable diesel and biojet occurs in Europe, which trying to shift the feedstock from palm oil to wastes, residues and rapeseed oil, while Brazilian biojet relies on soybean oil. In Indonesia, there is a blending mandates entitled B30 consisting of fossil fuel and biofuel in 70 : 30 proportion, which boosts the biofuel consumption that generated majorly from palm oil.

In summary, the biojet fuel is forecasted to develop swiftly in the near future, followed by the research improvement in this area. This phenomenon is also supported by the result of bibliometric analysis showing the increasing number of articles aligned to green diesel. For instance, about 33 articles was published in the beginning of 2023.

11. Conclusions

The favoured pathway on green diesel production through deoxygenation depended upon several factors including temperature, hydrogen pressure and catalyst. High temperature preferred DCO/DCO_2 owing to the high energy requirement for C–C cleavage and rich hydrogen environment directed the reaction towards HDO. In regards of catalyst, the reaction route was determined by two main categories: metal catalyst and support. Type of metal, metal area, and dispersion involved in the selectivity of the route. The characteristic of catalyst support was represented by the availability of Lewis acid sites, porosity and metal–support interaction.

Author contributions

Conceptualization: Hamzah Fansuri. Writing – original draft: Zeni Rahmawati, Liangga Santoso, Nor Laili Azua Jamari. Writing-review and editing: Triyanda Gunawan and Alan McCue.

Conflicts of interest

There are no conflicts to declare.

Acknowledgements

The authors thank the Ministry of Education, Culture, Research, and Technology Republik Indonesia for the research grant through the Penelitian Dasar Kompetitif Nasional scheme under main contract No. 084/E5/PG.02.00.PT/2022, and Researcher's Contract No. 1371/PKS/ITS/2022.

References

1 D. R. Dunn, J. Zaidi, M. Kopalek, G. Long, R. Berry G. McGrath, T. Shear, M. Klein, A. Gorski, E. Harrison, L. Jamison and K. Nakolan, *Monthly Energy Review- August 2022*, Energy Information Administration, United States, 2022.
2 F. Millo, T. Vlachos and A. Piano, *Fuel*, 2021, **285**, 119092.
3 S. Manikandan, S. Vickram, R. Sirohi, R. Subbaiya, R. Y. Krishnan, N. Karmegam, C. Sumathijones, R. Rajagopal, S. W. Chang, B. Ravindran and M. K. Awasthi, *Bioresour. Technol.*, 2023, **372**, 128679.
4 S. Ding, M. J. Hülsey, J. Pérez-Ramírez and N. Yan, *Joule*, 2019, **3**, 2897–2929.
5 IRENA, *Reaching zero with renewables: Biojet fuels*, International Renewable Energy Agency, Abu Dhabi, 2022.
6 H. I. Mahdi, A. Bazargan, G. McKay, N. I. W. Azelee and L. Meili, *Chem. Eng. Res. Des.*, 2021, **174**, 158–187.
7 M. K. Shahid, A. Batool, A. Kashif, M. H. Nawaz, M. Aslam, N. Iqbal and Y. Choi, *J. Environ. Manage.*, 2021, **297**, 113268.
8 M. Ameen, M. T. Azizan, A. Ramli, S. Yusup and B. Abdullah, *Catal. Today*, 2020, **355**, 51–64.
9 M. Makcharoen, A. Kaewchada, N. Akkarawatkhoosith and A. Jaree, *Energy Convers. Manage.: X*, 2021, **12**, 100125.
10 B. Fattahi, M. Haghighi, B. Rahmanivahid and N. Vardast, *Chem. Eng. Res. Des.*, 2022, **183**, 411–423.
11 N. A. Abdul Razak, N.-A. Mijan, Y. H. Taufiq-Yap and D. Derawi, *J. Cleaner Prod.*, 2022, **366**, 132971.
12 P. S. D. Priya, Y. Verma, R. A. Muhal, C. Goswami and T. Singh, *Mater. Today: Proc.*, 2022, **48**, 1178–1184.
13 M. M. A. Aziz, K. A. Kassim, Z. Shokravi, F. M. Jakarni, H. Y. Liu, N. Zaini, L. S. Tan, A. B. M. S. Islam and H. Shokravi, *Renewable Sustainable Energy Rev.*, 2020, **119**, 109621.
14 H. Shokravi, Z. Shokravi, M. Heidarrezaei, H. C. Ong, S. S. Rahimian Koloor, M. Petrů, W. J. Lau and A. F. Ismail, *Chemosphere*, 2021, **285**, 131535.
15 C. Ngamcharussrivichai, P. Totarat and K. Bunyakiat, *Appl. Catal., A*, 2008, **341**, 77–85.
16 R. Piloto-Rodríguez, Y. Sánchez-Borroto, M. Lapuerta, L. Goyos-Pérez and S. Verhelst, *Energy Convers. Manage.*, 2013, **65**, 255–261.
17 C. Kordulis, K. Bourikas, M. Gousi, E. Kordouli and A. Lycourghiotis, *Appl. Catal., B*, 2016, **181**, 156–196.
18 V. T. da Silva and L. A. Sousa, in *The Role of Catalysis for the Sustainable Production of Bio-fuels and Bio-chemicals*, Elsevier, 2013, pp. 67–92.
19 S. N. Naik, V. V. Goud, P. K. Rout and A. K. Dalai, *Renewable Sustainable Energy Rev.*, 2010, **14**, 578–597.
20 G. Di Vito Nolfi, K. Gallucci and L. Rossi, *Int. J. Environ. Res. Public Health*, 2021, **18**, 13041.
21 H. K. Jeswani, A. Chilvers and A. Azapagic, *Proc. R. Soc. A*, 2020, **476**, 20200351.
22 U.S. Department of Energy, *Sustainable Aviation Fuel: Review of Technical Pathways Executive*, 2020.
23 S. Widiyanto, *presented in part at the ICAO Seminar on Alternative Fuels*, ICAO Headquarters, Montreal, 2017.
24 EBTKE Public Relation, *Ground Run Test of Bioavtur J2.4: Well Accomplished*, The Ministry of Energy and Mineral Resource Republic of Indonesia, 2021.
25 K. W. Cheah, S. Yusup, A. C. M. Loy, B. S. How, V. Skoulou and M. J. Taylor, *Mol. Catal.*, 2022, **523**, 111469.
26 N. Hongloi, P. Prapainainar and C. Prapainainar, *Mol. Catal.*, 2022, **523**, 111696.
27 F. T. Yani, H. Husin, Darmadi, S. Muhammad, F. Abnisa, Nurhazanah, F. Nasution and Erdiwansyah, *J. Cleaner Prod.*, 2022, **354**, 131704.

28 T. K. Vo, W.-S. Kim, S.-S. Kim, K. S. Yoo and J. Kim, *Energy Convers. Manage.*, 2018, **158**, 92–102.
29 Z. Cai, R. Liang, P. Yu, Y. Liu, Y. Ma, Y. Cao, K. Huang, L. Jiang and X. Bao, *Fuel Process. Technol.*, 2022, **226**, 107091.
30 P. Hellier, M. Talibi, A. Eveleigh and N. Ladommatos, *Proc. Inst. Mech. Eng., Part D*, 2018, **232**, 90–105.
31 Y. Zhou, J. Remón, Z. Jiang, A. S. Matharu and C. Hu, *Green Energy Environ.*, 2022, S2468025722000528.
32 Y. S. M. Altarazi, A. R. Abu Talib, J. Yu, E. Gires, M. F. Abdul Ghafir, J. Lucas and T. Yusaf, *Energy*, 2022, **238**, 121910.
33 N. Asikin-Mijan, J. M. Ooi, G. AbdulKareem-Alsultan, H. V. Lee, M. S. Mastuli, N. Mansir, F. A. Alharthi, A. A. Alghamdi and Y. H. Taufiq-Yap, *J. Cleaner Prod.*, 2020, **249**, 119381.
34 R. G. Kukushkin, P. M. Yeletsky, C. T. Grassin, B.-H. Chen, O. A. Bulavchenko, A. A. Saraev and V. A. Yakovlev, *Chem. Eng. J.*, 2020, **396**, 125202.
35 Y. Wongnongwa, S. Jungsuttiwong, M. Pimsuta, P. Khemthong and M. Kunaseth, *Chem. Eng. J.*, 2020, **399**, 125586.
36 D. Singh, K. A. Subramanian and S. K. Singal, *Appl. Energy*, 2015, **155**, 440–446.
37 K. B. Baharudin, N. Abdullah, Y. H. Taufiq-Yap and D. Derawi, *J. Cleaner Prod.*, 2020, **274**, 122850.
38 X. Lei, H. Xin, X. Du, H. Yang, Y. Zeng, L. Zhou, C. Juan, H. Zhang, D. Li and C. Hu, *Fuel*, 2022, **324**, 124548.
39 W. Nor Adira Wan Khalit, N. Asikin-Mijan, T. Shafirah Marliza, M. Safa-Gamal, M. Razali Shamsuddin, I. Nur Azreena, M. Izham Saiman and Y. H. Taufiq-Yap, *J. Anal. Appl. Pyrolysis*, 2022, **164**, 105505.
40 L. E. Oi, M.-Y. Choo, H. V. Lee, Y. H. Taufiq-Yap, C. K. Cheng and J. C. Juan, *Int. J. Hydrogen Energy*, 2020, **45**, 11605–11614.
41 X. Y. Ooi, L. E. Oi, M.-Y. Choo, H. C. Ong, H. V. Lee, P. L. Show, Y.-C. Lin and J. C. Juan, *Fuel Process. Technol.*, 2019, **194**, 106120.
42 M. Žula, M. Grilc and B. Likozar, *Chem. Eng. J.*, 2022, **444**, 136564.
43 K. W. Cheah, M. J. Taylor, A. Osatiashtiani, S. K. Beaumont, D. J. Nowakowski, S. Yusup, A. V. Bridgwater and G. Kyriakou, *Catal. Today*, 2020, **355**, 882–892.
44 J. E. Lam, A. R. Mohamed, A. N. Kay Lup and M. K. Koh, *Fuel Process. Technol.*, 2022, **236**, 107394.
45 E. Santillan-Jimenez, T. Morgan, J. Shoup, A. E. Harman-Ware and M. Crocker, *Catal. Today*, 2014, **237**, 136–144.
46 N. Arun, R. V. Sharma and A. K. Dalai, *Renewable Sustainable Energy Rev.*, 2015, **48**, 240–255.
47 M.-Y. Choo, L. E. Oi, T. C. Ling, E.-P. Ng, Y.-C. Lin, G. Centi and J. C. Juan, *J. Anal. Appl. Pyrolysis*, 2020, **147**, 104797.
48 N. Asikin-Mijan, N. A. Rosman, G. AbdulKareem-Alsultan, M. S. Mastuli, H. V. Lee, N. Nabihah-Fauzi, I. M. Lokman, F. A. Alharthi, A. A. Alghamdi, A. A. Aisyahi and Y. H. Taufiq-Yap, *Process Saf. Environ. Prot.*, 2020, **142**, 336–349.
49 A. Yıldız, J. L. Goldfarb and S. Ceylan, *Fuel*, 2020, **263**, 116750.
50 D.-P. Phan and E. Y. Lee, *J. Catal.*, 2020, **386**, 19–29.
51 P. Šimáček and D. Kubička, *Fuel*, 2010, **89**, 1508–1513.
52 B. Veriansyah, J. Y. Han, S. K. Kim, S.-A. Hong, Y. J. Kim, J. S. Lim, Y.-W. Shu, S.-G. Oh and J. Kim, *Fuel*, 2012, **94**, 578–585.
53 A. Srifa, N. Viriya-empikul, S. Assabumrungrat and K. Faungnawakij, *Catal. Sci. Technol.*, 2015, **5**, 3693.
54 C. Hu, D. Creaser, S. Siahrostami, H. Grönbeck, H. Ojagh and M. Skoglundh, *Catal. Sci. Technol.*, 2014, **4**, 2427–2444.
55 X. Cao, J. Zhao, F. Long, P. Liu, X. Jiang, X. Zhang, J. Xu and J. Jiang, *Appl. Catal., B*, 2022, **312**, 121437.
56 M. de Oliveira Camargo, J. L. Castagnari Willimann Pimenta, M. de Oliveira Camargo and P. A. Arroyo, *Fuel*, 2020, **281**, 118719.
57 J. L. C. W. Pimenta, M. de Oliveira Camargo, R. Belo Duarte, O. A. A. dos Santos and L. M. de Matos Jorge, *Fuel*, 2021, **290**, 119979.
58 M. F. Wagenhofer, E. Baráth, O. Y. Gutiérrez and J. A. Lercher, *ACS Catal.*, 2017, **7**, 1068–1076.
59 F. Deng, J. Huang, E. E. Ember, K. Achterhold, M. Dierolf, A. Jentys, Y. Liu, F. Pfeiffer and J. A. Lercher, *ACS Catal.*, 2021, **11**, 14625–14634.
60 S. Fu, D. Li, T. Liu, L. Liu, H. Yang and C. Hu, *Catalysts*, 2022, **12**, 569.
61 N. Asikin-Mijan, H. V. Lee, J. C. Juan, A. R. Noorsaadah and Y. H. Taufiq-Yap, *RSC Adv.*, 2017, **7**, 46445–46460.
62 H. Yang, Y. Zeng, Y. Zhou, X. Du, D. Li and C. Hu, *J. Catal.*, 2022, **413**, 297–310.
63 Y. Bie, J. Lehtonen and J. Kanervo, *Appl. Catal., A*, 2016, **526**, 183–190.
64 J. Chen and Q. Xu, *Catal. Sci. Technol.*, 2016, **6**, 7239–7251.
65 S.-U. Lee, E. S. Kim, T.-W. Kim, J.-R. Kim, K.-E. Jeong, S. Lee and C.-U. Kim, *J. Ind. Eng. Chem.*, 2020, **83**, 366–374.
66 Y. Zhou, X. Liu, P. Yu and C. Hu, *Fuel*, 2020, **278**, 118295.
67 K. N. Papageridis, N. D. Charisiou, S. Douvartzides, V. Sebastian, S. J. Hinder, M. A. Baker, S. AlKhoori, K. Polychronopoulou and M. A. Goula, *Renewable Energy*, 2020, **162**, 1793–1810.
68 R. S. R. M. Hafriz, N. A. Arifin, A. Salmiaton, R. Yunus, Y. H. Taufiq-Yap, N. M. Saifuddin and A. H. Shamsuddin, *Fuel*, 2022, **308**, 122041.
69 B. Rozmysłowicz, P. Mäki-Arvela, S. Lestari, O. A. Simakova, K. Eränen, I. L. Simakova, D. Yu. Murzin and T. O. Salmi, *Top. Catal.*, 2010, **53**, 1274–1277.
70 P. Šimáček, D. Kubička, G. Šebor and M. Pospíšil, *Fuel*, 2009, **88**, 456–460.
71 H. Yan, S. Yao, T. Zhang, D. Li, X. Tang, M. Chen, Y. Zhou, M. Zhang, Y. Liu, X. Zhou, X. Feng, X. Chen and C. Yang, *Appl. Catal., B*, 2022, **306**, 121138.
72 S. T. Mohammed, K. I. Hamad, S. A. Gheni, D. Y. Aqar, S. M. R. Ahmed, M. A. Mahmood, S. Ceylan and G. H. Abdullah, *Chem. Eng. Sci.*, 2022, **251**, 117489.
73 F. Pinto, S. Martins, M. Gonçalves, P. Costa, I. Gulyurtlu, A. Alves and B. Mendes, *Appl. Energy*, 2013, **102**, 272–282.
74 M. Snåre, I. Kubičková, P. Mäki-Arvela, K. Eränen, J. Wärnå and D. Y. Murzin, *Chem. Eng. J.*, 2007, **134**, 29–34.

75 M. Arend, T. Nonnen, W. F. Hoelderich, J. Fischer and J. Groos, *Appl. Catal., A*, 2011, **399**, 198–204.
76 H. Bernas, K. Eränen, I. Simakova, A. R. Leino, K. Kordás, J. Myllyoja, P. Mäki-Arvela, T. Salmi and D. Y. Murzin, *Fuel*, 2010, **89**, 2033–2039.
77 M. Jin and M. Choi, *Mol. Catal.*, 2019, **474**, 110419.
78 J. L. F. Oliveira, L. M. B. Batista, N. Alburquerque dos Santos, A. M. M. Araújo, V. J. Fernandes, A. S. Araujo, A. P. M. Alves and A. D. Gondim, *Renewable Energy*, 2021, **168**, 1377–1387.
79 K. Praserttaweeporn, T. Vitidsant and W. Charusiri, *Results Eng.*, 2022, **14**, 100461.
80 M. Safa-Gamal, N. Asikin-Mijan, M. Arumugam, W. N. A. W. Khalit, I. Nur Azreena, F. S. Hafez and Y. H. Taufiq-Yap, *J. Anal. Appl. Pyrolysis*, 2021, **160**, 105334.
81 B. H. Susanto, M. Nasikin, Sukirno and A. Wiyo, *Procedia Chem.*, 2014, **9**, 139–150.
82 P. Šimáček, D. Kubička, I. Kubičková, F. Homola, M. Pospíšil and J. Chudoba, *Fuel*, 2011, **90**, 2473–2479.
83 C. Miao, O. Marin-Flores, S. D. Davidson, T. Li, T. Dong, D. Gao, Y. Wang, M. Garcia-Pérez and S. Chen, *Fuel*, 2016, **166**, 302–308.
84 J. A. Capunitan and S. C. Capareda, *Fuel Process. Technol.*, 2014, **125**, 190–199.
85 J. Horáček, Z. Tišler, V. Rubáš and D. Kubička, *Fuel*, 2014, **121**, 57–64.
86 Q. Liu, H. Zuo, Q. Zhang, T. Wang and L. Ma, *Chin. J. Catal.*, 2014, **35**, 748–756.
87 S. Kovács, T. Kasza, A. Thernesz, I. W. Horváth and J. Hancsók, *Chem. Eng. J.*, 2011, **176–177**, 237–243.
88 I. Nur Azreena, H. L. N. Lau, N. Asikin-Mijan, M. A. Hassan, S. M. Izham, M. Safa Gamal, W. Nor Adira Wan Khalit, M. Arumugam, E. Kennedy, M. Stockenhuber and Y. H. Taufiq-Yap, *J. Anal. Appl. Pyrolysis*, 2022, **161**, 105406.
89 S. Ding, Y. Guo, M. J. Hülsey, B. Zhang, H. Asakura, L. Liu, Y. Han, M. Gao, J. Hasegawa, B. Qiao, T. Zhang and N. Yan, *Chem*, 2019, **5**, 3207–3219.
90 D. Kubička, J. Horáček, M. Setnička, R. Bulánek, A. Zukal and I. Kubičková, *Appl. Catal., B*, 2014, **145**, 101–107.
91 C. Detoni, F. Bertella, M. M. V. M. Souza, S. B. C. Pergher and D. A. G. Aranda, *Appl. Clay Sci.*, 2014, **95**, 388–395.
92 P. Mäki-Arvela, I. Kubickova, M. Snåre, K. Eränen and D. Y. Murzin, *Energy Fuels*, 2007, **21**, 30–41.
93 F. Wang, H. Xu, S. Yu, H. Zhu, Y. Du, Z. Zhang, C. You, X. Jiang and J. Jiang, *Renewable Energy*, 2022, **197**, 40–49.
94 X. Liu, M. Yang, Z. Deng, A. Dasgupta and Y. Guo, *Chem. Eng. J.*, 2021, **407**, 126332.
95 K. A. Rogers, J. Fu, Y. Xu and Y. Zheng, *Catal. Today*, 2022, S0920586122001249.
96 P. Arora, E. L. Grennfelt, L. Olsson and D. Creaser, *Chem. Eng. J.*, 2019, **364**, 376–389.
97 L. Fu, Y. Li, H. Cui, W. Ba and Y. Liu, *Appl. Catal., A*, 2021, **623**, 118258.
98 G. C. R. Silva and M. H. C. de Andrade, *Biomass Convers. Biorefin.*, 2021, **13**, 1843–1857.
99 J. G. Immer and H. H. Lamb, *Energy Fuels*, 2010, **24**, 5291–5299.
100 D. Kubička and L. Kaluža, *Appl. Catal., A*, 2010, **372**, 199–208.
101 J. Wang, X. Chen, X. Chen, C. Zhao, Y. Ling and C. Liang, *Sustainable Energy Fuels*, 2022, **6**, 3025–3034.
102 K. Jeništová, I. Hachemi, P. Mäki-Arvela, N. Kumar, M. Peurla, L. Čapek, J. Wärnå and D. Yu. Murzin, *Chem. Eng. J.*, 2017, **316**, 401–409.
103 S. Janampelli and S. Darbha, *Energy Fuels*, 2018, **32**, 12630–12643.
104 N. Asikin-Mijan, G. AbdulKareem-Alsultan, M. S. Mastuli, A. Salmiaton, M. Azuwa Mohamed, H. V. Lee and Y. H. Taufiq-Yap, *Fuel*, 2022, **325**, 124917.
105 H. Du, Q. Yu, G. Liu, J. Li, J. Zhang, W. Wang, G. Duan, Y. Meng and H. Xie, *Fuel*, 2022, **317**, 123367.
106 Z. Ding, T. Zhao, Q. Zhu, S. Liao, L. Ning, Y. Bi and H. Chen, *Biomass Bioenergy*, 2020, **143**, 105879.
107 W. Zhou, H. Xin, H. Yang, X. Du, R. Yang, D. Li and C. Hu, *Catalysts*, 2018, **8**, 153.
108 K.-W. Jeon, H.-R. Park, Y.-L. Lee, J.-E. Kim, W.-J. Jang, J.-O. Shim and H.-S. Roh, *Fuel*, 2022, **311**, 122488.
109 A. Galadima and O. Muraza, *J. Ind. Eng. Chem.*, 2015, **29**, 12–23.
110 S. Lestari, P. Mäki-Arvela, I. Simakova, J. Beltramini, G. Q. M. Lu and D. Yu. Murzin, *Catal. Lett.*, 2009, **130**, 48–51.
111 K. Hengst, M. Arend, R. Pfützenreuter and W. F. Hoelderich, *Appl. Catal., B*, 2015, **174–175**, 383–394.
112 J. Lu, M. Faheem, S. Behtash and A. Heyden, *J. Catal.*, 2015, **324**, 14–24.
113 T. Morgan, D. Grubb, E. Santillan-Jimenez and M. Crocker, *Top. Catal.*, 2010, **53**, 820–829.
114 E. S. K. Why, H. C. Ong, H. V. Lee, W.-H. Chen, N. Asikin-Mijan, M. Varman and W. J. Loh, *Energy*, 2022, **239**, 122017.
115 L. J. Konwar and J.-P. Mikkola, *Appl. Catal., A*, 2022, **638**, 118611.
116 R. Loe, K. Huff, M. Walli, T. Morgan, D. Qian, R. Pace, Y. Song, M. Isaacs, E. Santillan-Jimenez and M. Crocker, *Catalysts*, 2019, **9**, 200.
117 M. Oh, M. Jin, K. Lee, J.-C. Kim, R. Ryoo and M. Choi, *Chem. Eng. J.*, 2022, **439**, 135530.
118 A. Ali and C. Zhao, *Chin. J. Catal.*, 2020, **41**, 1174–1185.
119 L. Zhou, W. Lin, K. Liu, Z. Wang, Q. Liu, H. Cheng, C. Zhang, M. Arai and F. Zhao, *Catal. Sci. Technol.*, 2020, **10**, 222–230.
120 M. S. Gamal, N. Asikin-Mijan, W. N. A. W. Khalit, M. Arumugam, M. Izham Saiman and Y. H. Taufiq-Yap, *Fuel Process. Technol.*, 2020, **208**, 106519.
121 S. Janampelli and S. Darbha, *Catal. Today*, 2021, **375**, 174–180.
122 S. Thongkumkoon, W. Kiatkittipong, U. W. Hartley, N. Laosiripojana and P. Daorattanachai, *Renewable Energy*, 2019, **140**, 111–123.
123 C. Sarkar, S. Chandra Shit, D. Quang Dong, J. Lee, N. Han Tran, R. Singuru, K. An, N. Dang Nam, Q. Van Le, P. Nana Amaniampong, A. Drif, F. Jerome, P. Thanh Huyen, T. To Nga Phan, D.-V. N. Vo, N. Thanh Binh,

Q. Thang Trinh, M. P. Sherburne and J. Mondal, *Green Chem.*, 2020, **22**, 2049–2068.
124 S. Lestari, P. Mäki-Arvela, K. Eränen, J. Beltramini, G. Q. Max Lu and D. Yu. Murzin, *Catal. Lett.*, 2010, **134**, 250–257.
125 J. G. Immer, M. J. Kelly and H. H. Lamb, *Appl. Catal., A*, 2010, **375**, 134–139.
126 B. Rozmysłowicz, P. Mäki-Arvela, A. Tokarev, A.-R. Leino, K. Eränen and D. Yu. Murzin, *Ind. Eng. Chem. Res.*, 2012, **51**, 8922–8927.
127 E. Meller, U. Green, Z. Aizenshtat and Y. Sasson, *Fuel*, 2014, **133**, 89–95.
128 S. K. Kim, J. Y. Han, H. Lee, T. Yum, Y. Kim and J. Kim, *Appl. Energy*, 2014, **116**, 199–205.
129 A. Srifa, K. Faungnawakij, V. Itthibenchapong and S. Assabumrungrat, *Chem. Eng. J.*, 2015, **278**, 249–258.
130 L. Fu, Z. Liu, X. Li, Y. Li, H. Yang and Y. Liu, *Fuel*, 2022, **322**, 124027.
131 H. Wang, S. Yan, S. O. Salley and K. Y. Simon Ng, *Fuel*, 2013, **111**, 81–87.
132 A. A. Stepacheva, A. I. Sidorov, V. G. Matveeva, M. G. Sulman and E. M. Sulman, *Chem. Eng. Technol.*, 2019, **42**, 780–787.
133 Y. Zhou, L. Liu, G. Li and C. Hu, *ACS Catal.*, 2021, **11**, 7099–7113.
134 V. K. Soni, S. Dhara, R. Krishnapriya, G. Choudhary, P. R. Sharma and R. K. Sharma, *Fuel*, 2020, **266**, 117065.
135 M. Lin, X. Zhang, L. Zhan, X. Li, X. Song and Y. Wu, *Fuel*, 2022, **318**, 123605.
136 A. S. Berenblyum, R. S. Shamsiev, T. A. Podoplelova and V. Y. Danyushevsky, *Russ. J. Phys. Chem.*, 2012, **86**, 1199–1203.
137 A. S. Berenblyum, V. Y. Danyushevsky, E. A. Katsman, R. S. Shamsiev and V. R. Flid, *Pet. Chem.*, 2013, **53**, 362–366.
138 J. Liang, Z. Zhang, K. Wu, Y. Shi, W. Pu, M. Yang and Y. Wu, *Fuel Process. Technol.*, 2019, **188**, 153–163.
139 Z. Zhang, H. Chen, C. Wang, K. Chen, X. Lu, P. Ouyang and J. Fu, *Fuel*, 2018, **230**, 211–217.
140 S. Zulkepli, H. V. Lee, N. Abd. Rahman, L. T. Chuan, P. L. Show, W.-H. Chen and J. C. Juan, *Fuel*, 2022, **308**, 121860.
141 T. Thangadurai and C. T. Tye, *Period. Polytech., Chem. Eng.*, 2021, **65**, 350–360.
142 J. Bian, Y. Wang, Q. Zhang, X. Fang, L. Feng and C. Li, *RSC Adv.*, 2017, **7**, 47279–47287.
143 S. N. Zdainal Abidin, H. V. Lee, N. Asikin-Mijan, J. C. Juan, N. A. Rahman, M. S. Mastuli, Y. H. Taufiq-Yap and P. S. Kong, *Pure Appl. Chem.*, 2020, **92**, 587–600.
144 R. S. R. M. Hafriz, I. Nor Shafizah, A. Salmiaton, N. A. Arifin, R. Yunus, Y. H. Taufiq Yap and S. Abd Halim, *Arabian J. Chem.*, 2020, **13**, 8146–8159.
145 J. Zhong, Q. Deng, T. Cai, X. Li, R. Gao, J. Wang, Z. Zeng, G. Dai and S. Deng, *Fuel*, 2021, **292**, 120248.
146 G. C. R. Silva, D. Qian, R. Pace, O. Heintz, G. Caboche, E. Santillan-Jimenez and M. Crocker, *Catalysts*, 2020, **10**, 91.
147 N. A. Rashidi, E. Mustapha, Y. Y. Theng, N. A. A. Razak, N. A. Bar, K. B. Baharudin and D. Derawi, *Fuel*, 2022, **313**, 122695.
148 M. V. Tsodikov, A. V. Chistyakov, M. A. Gubanov, P. A. Zharova, S. S. Shapovalov, A. A. Pasynskii, V. V. Kriventsov and I. I. Moiseev, *Russ. Chem. Bull.*, 2015, **64**, 2062–2068.
149 N. Chen, Y. Ren and E. W. Qian, *J. Catal.*, 2016, **334**, 79–88.
150 X. Li, Q. Wang, J. Chen, S. Li, D. Wang and Z. Zheng, *J. Anal. Appl. Pyrolysis*, 2021, **156**, 105121.
151 P. A. Zharova, A. V. Chistyakov, S. S. Shapovalov, A. A. Pasynskii and M. V. Tsodikov, *Energy*, 2019, **172**, 18–25.
152 H. Shi, X. Gu, Y. Shi, D. Wang, S. Shu, Z. Wang and J. Chen, *Front. Chem. Sci. Eng.*, 2022, **17**, 139–155.
153 R. Loe, E. Santillan-Jimenez, T. Morgan, L. Sewell, Y. Ji, S. Jones, M. A. Isaacs, A. F. Lee and M. Crocker, *Appl. Catal., B*, 2016, **191**, 147–156.
154 A. V. Chistyakov, V. V. Kriventsov, A. V. Naumkin, A. Y. Pereyaslavtsev, P. A. Zharova and M. V. Tsodikov, *Pet. Chem.*, 2016, **56**, 607–615.
155 L. Zhao, B. Li and C. Zhao, *ACS Sustainable Chem. Eng.*, 2021, **9**, 12970–12977.
156 L. Chen, H. Li, J. Fu, C. Miao, P. Lv and Z. Yuan, *Catal. Today*, 2016, **259**, 266–276.
157 K. C. Kwon, H. Mayfield, T. Marolla, B. Nichols and M. Mashburn, *Renewable Energy*, 2011, **36**, 907–915.
158 C. H. Bartholomew and R. J. Farrauto, *Fundamentals of Industrial Catalytic Processes*, John Wiley & Sons, Inc., 2nd edn, 2006.
159 J. Cheng, Z. Zhang, X. Zhang, Z. Fan, J. Liu and J. Zhou, *Int. J. Hydrogen Energy*, 2019, **44**, 11765–11773.
160 F. P. Sousa, L. N. Silva, D. B. de Rezende, L. C. A. de Oliveira and V. M. D. Pasa, *Fuel*, 2018, **223**, 149–156.
161 B. F. Honorato de Oliveira, L. F. de França, N. C. Fernandes Corrêa, N. F. d. P. Ribeiro and M. Velasquez, *Catalysts*, 2021, **11**, 1088.
162 J. M. Crawford, C. S. Smoljan, J. Lucero and M. A. Carreon, *Catalysts*, 2019, **9**, 42.
163 M. Arroyo, L. Briones, H. Hernando, J. M. Escola and D. P. Serrano, *Energy Fuels*, 2021, **35**, 17167–17181.
164 P. Aiamsiri, D. Tumnantong, B. Yoosuk, C. Ngamcharussrivichai and P. Prasassarakich, *Energy Fuels*, 2021, **35**, 14793–14804.
165 H. Xin, H. Yang, X. Lei, X. Du, K. Zhou, D. Li and C. Hu, *Ind. Eng. Chem. Res.*, 2020, **59**, 17373–17386.
166 Z. Zhang, G. Bi, H. Zhang, A. Zhang, X. Li and J. Xie, *Fuel*, 2019, **247**, 26–35.
167 M. Liu, Y. Shi, K. Wu, J. Liang, Y. Wu, S. Huang and M. Yang, *Catal. Commun.*, 2019, **129**, 105726.
168 F. Wang, R. Pace, Y. Ji, J. Jiang, X. Jiang, A. Krystianiak, O. Heintz, G. Caboche, E. Santillan-Jimenez and M. Crocker, *Renewable Energy*, 2022, **195**, 1468–1479.
169 K. N. Papageridis, N. D. Charisiou, S. L. Douvartzides, V. Sebastian, S. J. Hinder, M. A. Baker, S. AlKhoori, K. Polychronopoulou and M. A. Goula, *Fuel Process. Technol.*, 2020, **209**, 106547.

170 T. Hengsawad, T. Jindarat, D. E. Resasco and S. Jongpatiwut, *Appl. Catal., A*, 2018, **566**, 74–86.
171 I.-H. Choi, J.-S. Lee, C.-U. Kim, T.-W. Kim, K.-Y. Lee and K.-R. Hwang, *Fuel*, 2018, **215**, 675–685.
172 X. Li, X. Yang, Q. Wang, S. Li, Y. Ye, D. Wang and Z. Zheng, *J. Cleaner Prod.*, 2022, **350**, 131520.
173 W. N. A. W. Khalit, N. Asikin-Mijan, T. S. Marliza, M. S. Gamal, M. R. Shamsuddin, M. I. Saiman and Y. H. Taufiq-Yap, *Biomass Bioenergy*, 2021, **154**, 106248.
174 N. Aliana-Nasharuddin, N. Asikin-Mijan, G. Abdulkareem-Alsultan, M. I. Saiman, F. A. Alharthi, A. A. Alghamdi and Y. H. Taufiq-Yap, *RSC Adv.*, 2020, **10**, 626–642.
175 G. Abdulkareem-Alsultan, N. Asikin-Mijan, L. K. Obeas, R. Yunus, S. Z. Razali, A. Islam and Y. Hin Taufiq-Yap, *Chem. Eng. J.*, 2022, **429**, 132206.
176 M. S. Gamal, N. Asikin-Mijan, W. N. A. W. Khalit, M. Arumugam, S. M. Izham and Y. H. Taufiq-Yap, *Fuel Process. Technol.*, 2020, **208**, 106519.
177 IPCC, *Climate Change 2022: Mitigation of Climate Change. Contribution of Working Group III to the Sixth Assessment Report of the Intergovernmental Panel on Climate Change*, Cambridge University Press, Cambridge, 2022.
178 IRENA, *World Energy Transitions Outlook 2022: 1.5 °C Pathway – Executive Summary*, International Renewable Energy Agency, Abu Dhabi, 2022.
179 ICAO, *Climate Change Mitigation: Overview*, The International Civil Association, 2022.
180 IEA, *Renewables 2022: Analysis and forecast to 2027*, International Energy Agency, 2022.